

## Reactivity of periodically rippled graphene grown on Ru(0001)

This article has been downloaded from IOPscience. Please scroll down to see the full text article.

2009 J. Phys.: Condens. Matter 21 134002

(<http://iopscience.iop.org/0953-8984/21/13/134002>)

View [the table of contents for this issue](#), or go to the [journal homepage](#) for more

Download details:

IP Address: 129.252.86.83

The article was downloaded on 29/05/2010 at 18:47

Please note that [terms and conditions apply](#).

# Reactivity of periodically rippled graphene grown on Ru(0001)

B Borca<sup>1</sup>, F Calleja<sup>1</sup>, J J Hinarejos<sup>1</sup>, A L Vázquez de Parga<sup>1,2</sup> and R Miranda<sup>1,2</sup>

<sup>1</sup> Departamento de Física de la Materia Condensada, Universidad Autónoma de Madrid, Cantoblanco, E-28049 Madrid, Spain

<sup>2</sup> Instituto Madrileño de Estudios Avanzados en Nanociencia (IMDEA Nanociencia), Cantoblanco, E-28049 Madrid, Spain

Received 21 November 2008, in final form 28 December 2008

Published 12 March 2009

Online at [stacks.iop.org/JPhysCM/21/134002](http://stacks.iop.org/JPhysCM/21/134002)

## Abstract

We report here the reactivity of epitaxial graphene islands and complete monolayers on Ru(0001) towards molecular oxygen and air. The graphene is prepared by thermal decomposition of ethylene molecules pre-adsorbed on an Ru(0001) surface in an ultra-high vacuum chamber. The graphene layer presents a periodically rippled structure that is dictated by the misfit between graphene and Ru(0001) lattice parameters. The periodic ripples produce spatial charge redistribution in the graphene and modifies its electronic structure around the Fermi level. In order to investigate the reactivity of graphene we expose graphene islands to a partial pressure of oxygen and following the evolution of the surface by STM during the exposure. For the exposure to air we removed the sample from the UHV chamber and we re-introduce it after several hours, taking STM images before and after. The surface areas not covered by the graphene islands present a dramatic change but the graphene structure, even the borders of the islands, remain intact. In the case of a complete graphene monolayer the exposure to oxygen or to air does not affect or destroy the rippled structure of the graphene monolayer.

(Some figures in this article are in colour only in the electronic version)

## 1. Introduction

The recent discovery of an experimental method to prepare graphene [1] enforced the research field, stimulating new discoveries [2–4] and potential applications [5–7] based principally on the exceptional electronic properties [8] of the graphene layer. Single or few layers of graphene can be prepared by micromechanical cleavage [1] or chemical exfoliation of highly oriented pyrolytic graphite [9], thermal decomposition of SiC [10, 11], or epitaxially by chemical vapor deposition of hydrocarbons on metal substrate [12, 13]. The growth of graphene layers on different substrates modifies the electronic structure by either doping the graphene layer with electrons or holes, or inducing a periodic modulation in the density of states, or both effects simultaneously [14–16]. It is an open question how these modifications in the electronic structure could change some of the unique properties of graphene.

It has been proposed and demonstrated that graphene deposited in silicon oxide could be used as a gas detector

even for a single molecule [7]. Very recently a theoretical study using first-principles calculations explored the optimal adsorption position and orientation of different molecules (H<sub>2</sub>O, NH<sub>3</sub>, CO, NO<sub>2</sub>, NO) on self-standing graphene layers. A graphene layer grown on an Ni(111) surface has been used to protect the crystal surface from oxidation when exposed to molecular oxygen [17]. The authors not only checked that the graphene layer prevents the oxidation of the Ni(111) surface but also measured that the emission of spin-polarized secondary electrons from the Ni(111) surface was not affected by the presence of the graphene overlayer [17]. Graphene and Ni(111) have exactly the same lattice parameter and therefore all the carbon atoms on the surface are equivalent and the main influence of the substrate in this system is to dope the graphene overlayer with electrons moving the Dirac point below the Fermi energy [16].

In this paper we present an investigation of the reactivity of epitaxial graphene on Ru(0001) towards exposure to pure oxygen inside an ultra-high vacuum (UHV) chamber and also exposing the crystal to air. Graphene and Ru(0001) have

different lattice parameters that induce a Moiré pattern in the graphene overlayer. This difference makes it that the registry, and therefore the hybridization between the carbon atoms and the ruthenium ones, changes inside the unit cell, introducing a modulation in the electronic structure. We would elucidate if this modification in the electronic structure affects the reactivity of graphene. We can produce either a continuous graphene layer or small islands with a wide size distribution. We exposed the different samples in UHV to molecular oxygen and by means of scanning tunneling microscopy (STM) we study the reactivity of the surface during the oxygen deposition. For the samples exposed to air we removed them from the UHV chamber and after several hours we re-introduced them into the chamber and we took STM images without any cleaning procedure.

## 2. Experimental procedures

The samples were prepared in a UHV chamber with a base pressure in the range of  $10^{-11}$  Torr. The chamber is equipped with a variable temperature STM microscope, a reverse view low energy electron diffraction (LEED) optics that allow us to do Auger spectroscopy, and facilities for ion sputtering, evaporation and gas exposure. The Ru(0001) crystal was cleaned by cycles of  $\text{Ar}^+$  sputtering and annealing followed by oxygen exposure and heating to high temperature [18]. The graphene continuous layers were produced by segregation of carbon from the Ru(0001) bulk and the sub-monolayer coverages by thermal decomposition at 1000 K of ethylene molecules pre-adsorbed at 300 K on the sample surface. The oxygen exposure was carried out by filling the UHV chamber with a partial oxygen pressure of  $1 \times 10^{-7}$  Torr for a given period of time following the evolution of the surface by STM during the exposure. The air exposure was performed by removing the sample from the UHV chamber and re-introducing it into the UHV for the STM measurements. All images were recorded in the constant current mode. The polycrystalline W STM tips were routinely cleaned *in situ* by ion sputtering and annealing by electron bombardment to make a ‘blunt’ tip with a featureless electronic structure around the Fermi level [19].

## 3. Results and discussion

### 3.1. Graphene monolayer

The graphene monolayer on Ru(0001) covers completely the surface reproducing the steps, dislocations and defects of the substrate as can be seen in figure 1. The graphene layer presents a hexagonal arrangement of protrusions. This superstructure can be understood as a Moiré pattern resulting from the superposition of two hexagonal lattices with different lattice parameters. The resulting superstructure presents an appropriate distance between protrusions of 2.7 nm. Within the unit cell the registry of the carbon atoms with respect to the ruthenium ones changes, which implies that the distance and hybridization between the graphene layer and the substrate is not uniform. The anisotropy in the interaction induces

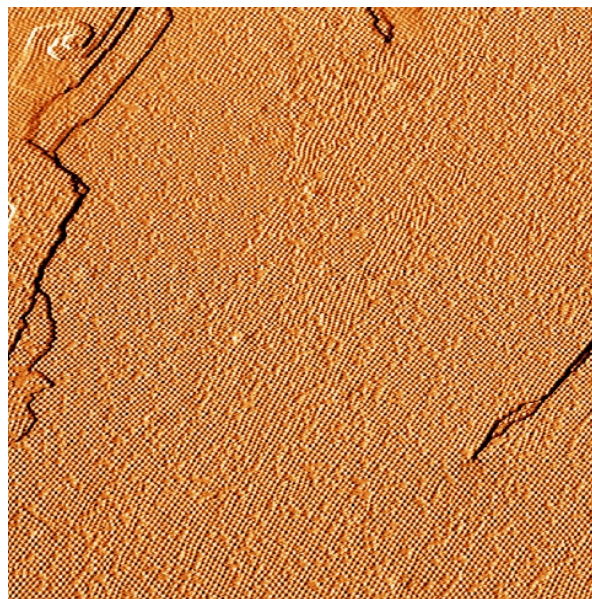


**Figure 1.** 400 nm  $\times$  400 nm STM image showing a monolayer of graphene covering completely the surface of the Ru(0001) crystal. The image was measured with a sample bias voltage  $V_s = -0.66$  V and a tunneling current  $I_t = 0.18$  nA. The topographic image is numerically differentiated along the X direction.

a spatial charge redistribution in the graphene with electron pockets in the upper part of the Moiré structure. This has been measured with spatially resolved  $dI/dV$  maps by means of scanning tunneling spectroscopy [15]. The influence of the electronic structure in the STM images is quite strong, as can be seen in figure 2. In the upper panel we show two STM images measured exactly in the same position but changing the bias voltage applied between tip and sample. As can be seen in the profile shown in figure 2(b) the corrugation of the graphene structure changes by a factor of two, changing the voltage from  $-1$  to  $+1$  V. In fact the apparent corrugation of the Moiré superstructure changes from 0.12 nm at  $-1$  V down to 0.02 nm at  $+2$  V and when the bias voltage applied between tip and sample is higher than  $+3$  V the contrast of the Moiré pattern is inverted. This proves that the electronic effects in this system are stronger than the actual geometric corrugation of the graphene layer. In fact, all the scanning tunneling spectroscopy data can be explained with a very simple tight-binding model using a flat graphene layer and applying an external potential with the periodicity of the Moiré pattern [15].

The presence of such strong electronic effects around the Fermi level in this system opens questions concerning the reactivity of this system. It has been shown that a flat graphene layer covering a Ni(111) crystal is completely inert towards exposure to molecular oxygen [17]. Graphene and Ni(111) have the same lattice parameters and therefore all carbon atoms on the graphene layer are equivalent. In our case the system presents a strong modulation in the electronic structure around the Fermi level and in order to test if this new electronic structure has any effect on the reactivity we exposed the graphene overlayer to molecular oxygen for 1 h at  $1 \times 10^{-6}$  Torr with the sample kept at 300 K while we measured

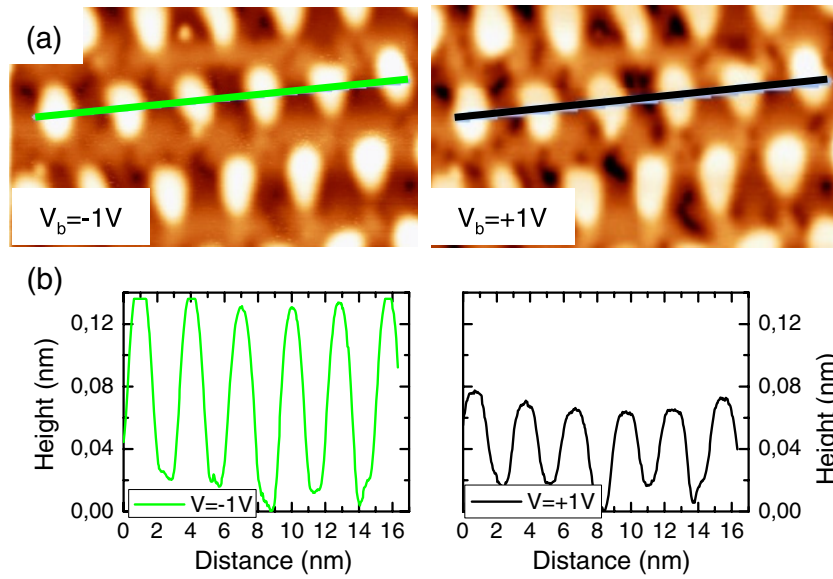


**Figure 2.** (a)  $18 \text{ nm} \times 8 \text{ nm}$  STM images measured with  $V_s = -1 \text{ V}$  (right) and  $V_s = +1 \text{ V}$  (left) in the same area. (b) Line profiles measured on the images shown in (a). The vertical scale on the line profiles is identical to allow a direct comparison between the apparent corrugation of the Moiré pattern.

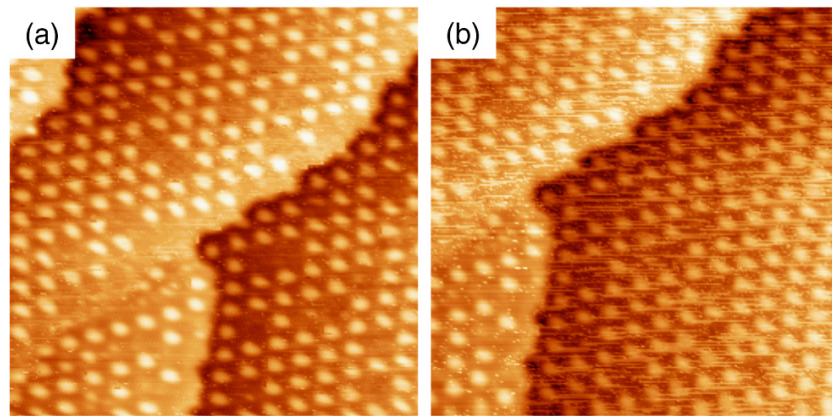


**Figure 3.**  $50 \text{ nm} \times 50 \text{ nm}$  STM images of graphene monolayer on Ru(0001) surface, recorded (a) before and (b) after 60 min of exposure to a partial pressure of molecular oxygen of  $1 \times 10^{-6}$  Torr. The images were taken with a sample bias voltage of  $V_s = -0.54 \text{ V}$  and a tunnel current of  $I_t = 0.2 \text{ nA}$ .

simultaneously with the STM. Figure 3 shows two snapshots of the movie recorded during the exposure. Figure 3(a) shows the graphene overlayer before the oxygen exposure covering the Ru(0001) substrates. The image shows three steps from the Ru(0001) substrate completely covered by the graphene overlayer. There are a few defects in the Moiré pattern, probably due to a small amount of contamination on the Ru(0001) surface. Figure 3(b) shows an image measured in the same area of the sample after 45 min of exposition. The only change visible in the images are horizontal lines probably due to oxygen atoms or  $\text{O}_2$  molecules diffusing along the graphene surface. This result shows the lack of reactivity towards oxygen exposure for the graphene layer grown on the Ru(0001) surface. Despite its new strongly modulated electronic structure around the Fermi level, the graphene shows a lack of reactivity. The same result was obtained after removing the sample from the UHV chamber and leaving it

in air for 12 h and re-introducing it into the UHV chamber through a fast load-lock entry (images not shown).

### 3.2. Graphene sub-monolayer

By reducing the amount of ethylene absorbed on the Ru(0001) surface we can produce nanometer-sized graphene islands. As can be seen in figure 4 we have a wide distribution in the size of the islands. Most of the islands have a quasi-hexagonal shape with straight edges that present a zig-zag structure [15]. The islands are one monolayer thick with an apparent distance between the lower part of the Moiré pattern and the Ru(0001) surface of  $0.14 \text{ nm} \pm 0.02 \text{ nm}$  for sample bias voltages between  $\pm 1 \text{ V}$  around the Fermi level [20]. This number is in good agreement with the average interlayer distance found by low energy electron diffraction [21].

When a graphene sheet is cut two types of edges are produced known as armchair and zig-zag. Previous theoretical





**Figure 4.** 750 nm  $\times$  750 nm STM image of graphene islands on Ru(0001) stepped surface. The image was taken with a sample bias voltage of  $V_s = -0.9$  V and a tunnel current of  $I_t = 0.1$  nA. The topographic image is numerically differentiated along the X direction.

work [22, 23] on the electronic structure of finite graphite systems has shown that graphite with zig-zag edges has a localized edge state at the Fermi level, but those with armchair

edges have no such state. For graphene the same result is true and the edge state appears at the Fermi level on the zig-zag edges. The corresponding energy bands are almost flat and thereby produce a sharp peak in the density of states [23]. These edge states are spatially localized at the carbon atoms on the edge sites. In recent theoretical work the reactivity of the zig-zag edges has been explored examining the reaction energetics with common radicals (H, OH, CH<sub>3</sub>, F, Cl, Br, I) using first-principles calculations [24].

In order to investigate the reactivity of graphene islands on Ru(0001) we exposed them to a partial pressure of oxygen and we follow the evolution of the surface by STM during the exposure. It is well known that exposure of a clean Ru(0001) surface to a partial pressure of oxygen leads to a dissociative chemisorption of oxygen and, in a first step, to a  $2 \times 2$  superstructure of oxygen atoms on the Ru(0001) surface [25, 18]. Figure 5 shows four snapshots from a movie taken while exposing the surface to oxygen. In figure 5(a) we show the edge of a graphene island before oxygen exposure. On the left-hand side of the image the clean Ru(0001) surface can be observed; the defect present on the surface (marked with an arrow) will be used as a marker in the following images. On the right-hand side of the image the Moiré pattern of the graphene island can be seen. All the images shown in this figure are differentiated along the horizontal direction to allow the detection of the faint depressions produced by the oxygen atoms on the Ru(0001) surface and at the same time we will be able to see any changes on the surface of the graphene island

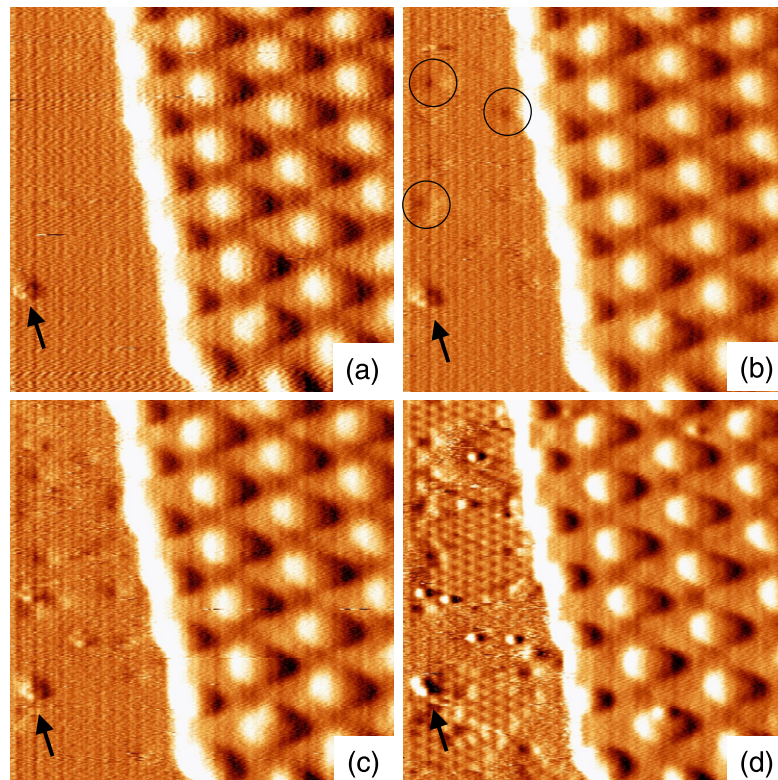


**Figure 5.** 17 nm  $\times$  17 nm STM images on the edge of a graphene island on Ru(0001) surface, recorded in real time (a) before and (b)–(d) during exposure to oxygen (3 min in a partial pressure of oxygen of  $5 \times 10^{-8}$  Torr). (b) Oxygen adsorption induces a  $2 \times 2$  superstructure on Ru(0001) while the graphene region and the edge are not affected. The images were taken with a sample bias voltage of  $V_s = -0.9$  V and a tunnel current of  $I_t = 0.1$  nA.

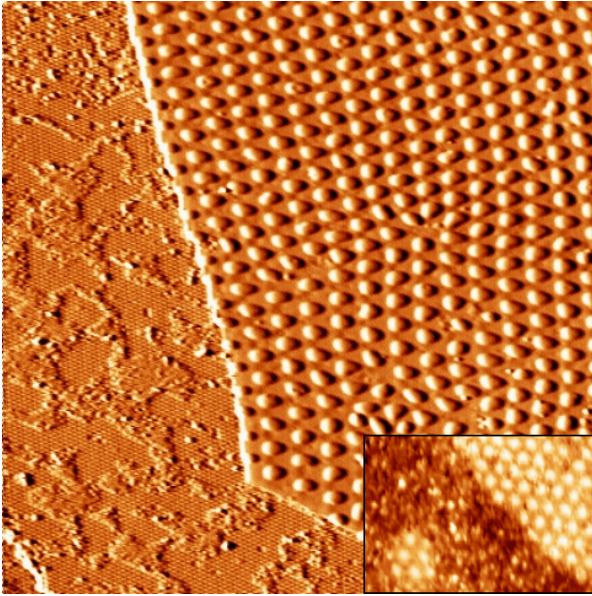


**Figure 6.** 75 nm  $\times$  75 nm STM image of the edge of a graphene island on Ru(0001) after exposing the surface for 7 min to  $5 \times 10^{-8}$  Torr. On the left-hand side of the image the Ru(0001) surface is covered with a  $2 \times 2$  superstructure formed by atomic oxygen. The unresolved patches that appear separating the  $2 \times 2$  areas are zones of the sample where the local oxygen coverage is higher and they present a  $2 \times 1$  superstructure [26]. The images have been differentiated along the  $X$  direction to increase the contrast in the  $2 \times 2$  superstructure. The images were recorded with a sample bias voltage  $V_s = -1.0$  V and a tunneling current  $I_t = 0.1$  nA. Inset: 48 nm  $\times$  33 nm STM image measured after exposing the surface for 12 h to air.

that is at least 0.14 nm higher. In figure 5(b) we show an image measured after 45 s of oxygen exposure. The surface of the graphene island remains unchanged but on the Ru(0001) surface we can see several small depressions (marked with black circles). We assign these small depressions to oxygen atoms diffusing on the Ru(0001) surface [18]. In figure 5(c) we show another image taken after a longer exposure to oxygen. As in the previous image on the graphene surface we cannot observe any change but on the Ru(0001) surface the number of depressions has increased. Finally in figure 5(d) we show the image measured after exposing the surface for 3 min to an oxygen partial pressure of  $5 \times 10^{-8}$  Torr. On the Ru(0001) surface we can observe the  $2 \times 2$  superstructure formed by the oxygen atoms separated by disordered areas where the oxygen coverage is higher and a  $2 \times 1$  superstructure is formed. In the STM images these areas appear disordered because the structure is not stable and the oxygen atoms exchange positions. On the surface of the graphene island we do not observe any change; even the edges of the islands remain intact. There is no change in this behavior upon increasing the oxygen partial pressure up to  $10^{-7}$  Torr or the exposure time.

The presence of the tip can shade the surface under it from the oxygen, reducing locally the exposure of the surface. Furthermore, the electric field between tip and sample in the area scanned may also modified the reactivity or diffusivity of the oxygen. To check out that this is not the case after exposing the surface to atomic oxygen we move the tip to a completely different area on the surface and we took several images to

confirm that our findings are not altered by the presence of the tip. In figure 6 we show a typical STM image measured after oxygen exposure on a non-canned area of the surface. The image shows the edge of a graphene island: on the left-hand side the oxygen is absorbed on the Ru(0001) surface forming the well-known  $2 \times 2$  superstructure (as can be seen in the image) [18]. The unresolved patches that appear separating the  $2 \times 2$  areas are zones of the sample where the local oxygen coverage is higher and they present a  $2 \times 1$  superstructure [26]. This structure is more difficult to resolved because the structure is not stable, due to the repulsion between the oxygen atoms, and therefore at room temperature the shape and order of these areas is not stable. On the right-hand side the image shows partially the surface of one of the graphene islands, where the Moiré pattern remains intact, as expected from the experiments with the complete monolayer. The edge of the graphene island also remains intact despite the presence of atomic oxygen diffusing on the surface. One possible explanation for this result is that the graphene edges are already passivated by the hydrogen that exists in the stainless steel UHV chamber as residual gas or that they are self-reconstructed.

For the island-covered surface we performed the same experiment as that for the fully covered surface. We removed the sample from the UHV chamber and we kept it in air for 12 h. Afterwards the sample was re-introduced into the UHV chamber using a fast load-lock entry. The sample was then transferred to the STM without any cleaning procedure. As can be seen in the inset of figure 6 the surface area not covered by graphene was completely contaminated. In contrast the surface covered by the graphene islands was clean and presents an undisturbed Moiré pattern.

#### 4. Conclusion

In conclusion, we studied the reactivity of a complete monolayer of graphene and a sub-monolayer on Ru(0001) prepared by thermal decomposition of ethylene on the Ru(0001) surface. The samples were exposed, keeping the sample at room temperature, to partial pressures of oxygen in the UHV chamber or removed from the chamber, kept in air for several hours and re-introduced into the UHV chamber. We find out that the graphene superstructure was not affected by the gas exposure. Even for the sub-monolayer regime we did not find any chemical reactivity on the edges of the graphene islands. This result confirms that a graphene monolayer grown on Ru(0001) efficiently protects the surface of the single crystal from being contaminated.

#### Acknowledgments

Financial support by the Ministerio de Ciencia e Innovación through projects FIS 2007-61114, MAT 2006-13470, CONSOLIDER on Molecular Nanoscience and the Comunidad de Madrid through project NANOMAGNET S-0505/MAT-0194 is acknowledged. BB thanks the Comunidad de Madrid for financial support.



**References**

- [1] Novoselov K S, Geim A K, Morozov S V, Jiang D, Zhang Y, Dubonos S V, Grigorieva I V and Firsov A A 2004 *Science* **306** 666
- [2] Novoselov K S, Geim A K, Morozov S V, Jiang D, Katsnelson M I, Grigorieva I V, Dubonos S V and Firsov A A 2005 *Nature* **438** 197
- [3] Zhang Y, Tan Y-W, Stormer H L and Kim P 2005 *Nature* **438** 201
- [4] Tombros N, Jozsa C, Popinciuc M, Jonkman H T and van Wees B J 2007 *Nature* **448** 571
- [5] Bunch J S, van der Zande A M, Verbridge S S, Frank I W, Tanenbaum D M, Parpia J M, Craighead H G and McEuen P L 2007 *Science* **315** 490
- [6] Williams J R, DiCarlo L and Marcus C M 2007 *Science* **317** 638
- [7] Schedin F, Geim A K, Morozov S V, Hill E H, Blake P, Katsnelson M I and Novoselov K S 2007 *Nat. Mater.* **6** 652
- [8] Geim A K and Novoselov K S 2007 *Nat. Mater.* **6** 183
- [9] Stankovich S, Dikin D A, Dommett G H B, Kohlhaas K M, Zimney E J, Stach E A, Piner R D, Nguyen S T and Ruoff R S 2006 *Nature* **442** 282
- [10] Forbeaux I, Themlin J-M and Debever J-M 1998 *Phys. Rev. B* **58** 16396
- [11] Berger C, Song Z, Li X, Wu X, Brown N, Naud C, Mayou D, Li T, Hass J, Marchenkov A N, Conrad E H, First P N and de Heer W A 2006 *Science* **312** 1191
- [12] Land T A, Michely T, Behm R J, Hemminger J C and Comsa G 1992 *Surf. Sci.* **264** 261
- [13] Oshima Ch and Nagashima A 1997 *J. Phys.: Condens. Matter* **9** 1
- [14] Zhou S Y, Gweon G-H, Fedorov A V, First P N, de Heer W A, Lee D-H, Guinea F, Castro Neto A H and Lanzara A 2007 *Nat. Mater.* **6** 770
- [15] Vázquez de Parga A L, Calleja F, Borca B, Passeggi M C G Jr, Hinarejos J J, Guinea F and Miranda R 2008 *Phys. Rev. Lett.* **100** 056807
- [16] Grüneis A and Vyalikh D V 2008 *Phys. Rev. B* **77** 193401
- [17] Dedkov Yu S, Fonin M and Laubschat C 2008 *Appl. Phys. Lett.* **92** 052506
- [18] Calleja F, Arnau A, Hinarejos J J, Vázquez de Parga A L, Hofer W A, Echenique P M and Miranda R 2004 *Phys. Rev. Lett.* **92** 206101
- [19] Vázquez de Parga A L, Hernán O S, Miranda R, Levy Yeyati A, Mingo N, Martí-Rodero A and Flores F 1998 *Phys. Rev. Lett.* **80** 357
- [20] Vázquez de Parga A L, Calleja F, Borca B, Passeggi M C G Jr, Hinarejos J J, Guinea F and Miranda R 2008 *Phys. Rev. Lett.* **101** 099704
- Vázquez de Parga A L, Calleja F, Borca B, Passeggi M C G Jr, Hinarejos J J, Guinea F and Miranda R 2008 *Phys. Rev. Lett.* **101** 099704
- [21] Sutter P W, Flege J-I and Sutter E A 2008 *Nat. Mater.* **7** 406
- [22] Fujita M, Wakabayashi K, Nakada K and Kusakabe K 1996 *J. Phys. Soc. Japan.* **65** 1920
- [23] Nakada K, Fujita M, Dresselhaus G and Dresselhaus M S 1996 *Phys. Rev. B* **54** 17954
- [24] Jiang D-E, Sumpter B G and Dai S 2007 *J. Chem. Phys.* **126** 134701
- [25] Wintterlin J, Trost J, Renisch S, Schuster R, Zambelli T and Ertl G 1997 *Surf. Sci.* **349** 159
- [26] Corriol C, Calleja F, Arnau A, Hinarejos J J, Vázquez de Parga A L, Hofer W A and Miranda R 2005 *Chem. Phys. Lett.* **405** 131